This article has been accepted for publication in a future issue of this journal, but has not been fully edited. Content may change prior to final publication. Citation information: DOI 10.1109/TIA.2019.2930433, IEEE Transactions on Industry Applications

Analysis of Switch Automation Based on Active Reconfiguration Considering Reliability, Energy Storage Systems and Variable Renewables

Sérgio F. Santos, Desta Z. Fitiwi, *Member, IEEE*, Marco R. M. Cruz, Cláudio Santos, and João P. S. Catalão, *Senior Member, IEEE*

***Abstract*—Economic development and changing lifestyles are leading to the extensive use of energy-intensive technologies by consumers. As a result, this has led to a dramatically increased demand for electricity. In addition, the consumers' increasing demand for a more reliable and uninterrupted energy supply is posing enormous challenge for service providers. This necessitates the development of novel solutions that should be at the system operators' disposal, particularly at distribution levels. One way to partly address this concern is by automating distribution systems and equipping them with intelligent technologies–a transformation to Smart Distribution Systems (SDSs). Such a transformation should improve system reliability and operational efficiency because such systems will be capable of operating and immediately restoring discontinued service to consumers. To facilitate this, it is necessary to replace manual switches by remotely controlled ones, improving the system restoration capability, which is one of the key features of smart grids. This paper presents a new framework to determine the minimal set of switches that have to be replaced or optimally allocated in order to automate the system. This is supported by a sensitivity analysis. Different topologies are also assessed taking into account various reliability indices and power losses in system operation following the system's automation. Such an optimization work is done under a massive integration of renewable energy sources and energy storage systems. All this simultaneously addresses the economic and functional requirements of the automated system, ultimately improving system's reliability. The standard IEEE 119-bus standard system is used as a case study, where different types of loads are considered (residential, commercial and industrial).**

***Index Terms*—Distribution Automation, Distributed Smart Systems, Reliability, Self-healing, Smart Grid, Service Restauration**

I. NOMENCLATURE

A. Sets/Indices

s/Ω^s	Index/set of scenarios
h/Ω^h	Index/set of hours
g/Ω^g	Index/set of generators
es/Ω^{es}	Index/set of energy storage
$\varsigma/\Omega^{\varsigma}$	Index/set of substations
l/Ω^l	Index/set of lines

B. Parameter

SW_l	Switching cost of each branch (
g_l, b_l, S_l^{max}	Conductance, susceptance and flow limit boundaries of each branch *l* (S, S, MVA)
R_l, X_l	Resistance, Reactance (Ω, Ω)
MP_l, MQ_l	Big-M parameters related with active and reactive power flows over each branch *l*
ρ_s	Probability of scenario *s*
OC_g	Cost of unit energy production
λ^{CO_2}	Emission rate imported power
λ^{ς}	Electricity price at the substation level (€/MWh)
ER_g^{DG}	Emission rate of DGs
ER_{ς}^{SS}	Emission rate of energy purchased from substation
$PD_{s,h}^n$	Demand at node *n* (MW)
$QD_{s,h}^n$	Reactive demand at node *n* (MVAr)
V_{nom}	Nominal voltage (kV)
η_{es}^{ch}	Charging efficiency
η_{es}^{dch}	Discharging efficiency
$E_{es,n}^{min}, E_{es,n}^{max}$	Energy Storage limit
μ_{es}	Scaling factor
$P_{g,n,s,h}^{DG,min}$, $P_{g,n,s,h}^{DG,max}$	Power generation limits (MW)
pf_g	Power factor of DG's
pf_{ss}	Power factor of substation
$P_{solar,h}$	Hourly solar PV power output (MW)
P_r	Rated power of RES unit (MW)
$P_{wind,h}$	Hourly wind power output (MW)
v_{ci}	Cut-in wind power (m/s)
v_{co}	Cut-out wind speed (m/s)
v_h	Hourly wind speed (m/s)
R_c	Certain radian point (usually 150W/m^2)
R_h	Hourly solar radiation (W/m^2)
R_{std}	Standard condition of solar radiation (usually 1000W/m^2)

C. Variables

$P_{\varsigma,s,h}^{SS}$, $Q_{\varsigma,s,h}^{SS}$	Imported power from grid (MW, MVAr)
$E_{es,n,s,h}$	Reservoir level of ESS (MWh)
$I_{es,n,s,h}^{dch}$, $I_{es,n,s,h}^{ch}$	Charging and discharging binary variables
$P_{g,n,s,h}^{DG}$, $Q_{g,n,s,h}^{DG}$	DG power (MW, MVAr)
$P_{\varsigma,n,s,h}^{SS}$	Imported power from grid (MW)

J.P.S. Catalão acknowledges the support by FEDER funds through COMPETE 2020 and by Portuguese funds through FCT, under POCI-01-0145-FEDER-029803 (02/SAICT/2017). D.Z. Fitiwi acknowledges support by a research grant from the Science Foundation Ireland (SFI) under the SFI Strategic Partnership Programme Grant number SFI/15/SPP/E3125. The opinions, findings and conclusions or recommendations expressed in this material are those of the authors and do not necessarily reflect the views of the SFI.

S.F. Santos is with INESC TEC, Porto 4200-465, Portugal (e-mail: sdfsantos@gmail.com).

D.Z. Fitiwi is with the Economic and Social Research Institute, and Trinity College Dublin, Dublin, Ireland (e-mail: desta.fitiwi@esri.ie).

M.R.M. Cruz is with C-MAST, University of Beira Interior, Covilhã 6201-001, Portugal (e-mail: marco.r.m.cruz@gmail.com).

C. Santos is with the Faculty of Engineering of the University of Porto, Porto 4200-465, Portugal (e-mail: cmmps95@gmail.com).

J.P.S. Catalão is with the Faculty of Engineering of the University of Porto and INESC TEC, Porto 4200-465, Portugal (e-mail: catalao@fe.up.pt).

This article has been accepted for publication in a future issue of this journal, but has not been fully edited. Content may change prior to final publication. Citation information: DOI 10.1109/TIA.2019.2930433, IEEE Transactions on Industry Applications

P_l, Q_l, θ_l	Active and reactive power flows respectively, and voltage angle difference of branch l (MW, MVAr, radians)
PL_l, PL_l	Active and reactive power losses of each branch l (MW, MVAr)
$P_{n,s,h}^{NS}$	Unserved active power at bus i (MW)
$Q_{n,s,h}^{NS}$	Unserved reactive power at bus i (MVAr)
V_i, V_j	Voltage magnitudes at bus i and j (kV)
$u_{l,h}$	Switching (binary) variables of existing branches
θ_i, θ_j	Voltage angle at node i and j (radians)
$x_{l,h}$	Binary variable to indicate line status
$y_{l,h}^{+}, y_{l,h}^{-}$	Auxiliary variables to indicate the status of a line
$\Delta V_{n,s,h}$	Voltage deviation magnitude (kV)
$\chi_{l,h}$	Binary switching variable of line l
$f_{l,h}$	Fictitious current flows through line l
$g_{n,h}^{SS}$	Fictitious current injections at substation nodes
$d_{n,h}$	Fictitious demand at a given node
n_{DG}	Number of candidate nodes for installation of distributed generation

D. Functions (in €)

SWC	Switching cost term (€)
TEC	Operation cost (€)
TENSC	Power not supplied cost (€)
TEmiC	Emissions cost (€)
EC_h^{DG}	Expected cost of energy produced by DGs (€)
EC_h^{ES}	Expected cost energy discharged from ESSs (€)
E_h^{SS}	Expected cost of energy imported through the substation level (€)
$EmiC_h^{DG}$	Expected emission cost due to DG power production (€)
$EmiC_h^{SS}$	Expected emission cost of energy imported through the substations (€)

II. Introduction

A. Background

In the face of increasing demand for electricity, ensuring the continuity of service is becoming a huge challenge in power systems. This is further exacerbated by the need for power systems to accommodate large-scale distributed energy resources such as renewable energy sources (RESs) and energy storage systems (ESSs) [1]–[3].

In general, in order to meet the aforementioned and other needs, existing electrical systems should evolve to a new paradigm of systems equipped with smart grid technologies and state-of-the-art solutions. Eventually, such systems are expected to effectively address the long-standing challenges of integrating clean but sporadic RESs, especially with regards to managing their inherent uncertainty and variability.

Without these measures, managing the intermittency of renewables may render impossible, especially with high penetrations, and service interruptions may be unavoidable.

Hence, in renewable-rich systems, maintaining continued service provision is under threat [4], [5]. As a result, the regulations on continuity of service need to evolve to improve the quality of service provision to residential, commercial and industrial customers and increase customer satisfaction [6]. Existing tools may not be sufficient; new and improved technological solutions will be required in order to ensure a standard level of service provision. Such solutions should be capable of maintaining high standards of service delivery and system restoration in case of failures.

Service failures and outages are inevitable in a distribution network systems during contingencies. Consequently, affected zones are momentarily disconnected and isolated from the rest of the grid. But solutions such as distribution system reconfiguration (DSR) can be used to restore as many loads as possible by redirecting power flows without violating the network's own operational constraints [7]–[9]. In an electrical power system, most failures occur in the distribution system, usually resulting in immediate service interruptions to the dismay of consumers. Traditionally, when the failure occurs and service stops, consumers call the respective distribution company. Upon receiving a service failure notification, a common practice is that a field crew is sent to search for the exact location of the fault, and isolate it via manual switches, and simultaneously restoring service to as many consumers as possible while repairing the failure [10]–[14]. Hence, in traditional distribution systems, such restoration and repairing processes are done manually by opening and/or closing switches. This usually takes longer time. However, with an automated system, restoration can be performed in a shorter time and even with fewer field crew members [12], [15]–[18].

One of the ways to perform system automatic restoration is by optimally positioning automated switches in distribution systems, and developing new technological solutions in order to improve the system's operational performance and restoration capability. It is widely accepted that remotely-controlled switches (RCSs) can substantially enhance the network's overall performance. The optimal functionalities of RCSs can be handled by the system operator in a distribution management center equipped with a DSR algorithm.

To enable remote control and management of distribution systems, it is mandatory to replace existing manual switches by RCSs as well as install new ones at optimal locations. All this improves the system's restoration capability, a positive contribution to reliability. However, this must be done in a most functional and economical way. The maximum restoration capability must be obtained by replacing and/or installing the minimum possible number of switches so as not to excessively increase investment costs [19]–[21].

As mentioned earlier, replacing the manual switches with these smart switches helps increase system reliability. The restoration process of distribution networks is an important aspect, and must be done as quickly as possible so as not to compromise the energy supply to consumers. In addition, it has been proven that RCSs bring more advantages in terms of adding more operational flexibility in the system, and speed of response to urgent and instant needs. However, it is not as simple as replacing all manual switches with RCSs; this can considerably expensive at both installation and maintenance levels.

This article has been accepted for publication in a future issue of this journal, but has not been fully edited. Content may change prior to final publication. Citation information: DOI 10.1109/TIA.2019.2930433, IEEE Transactions on Industry Applications

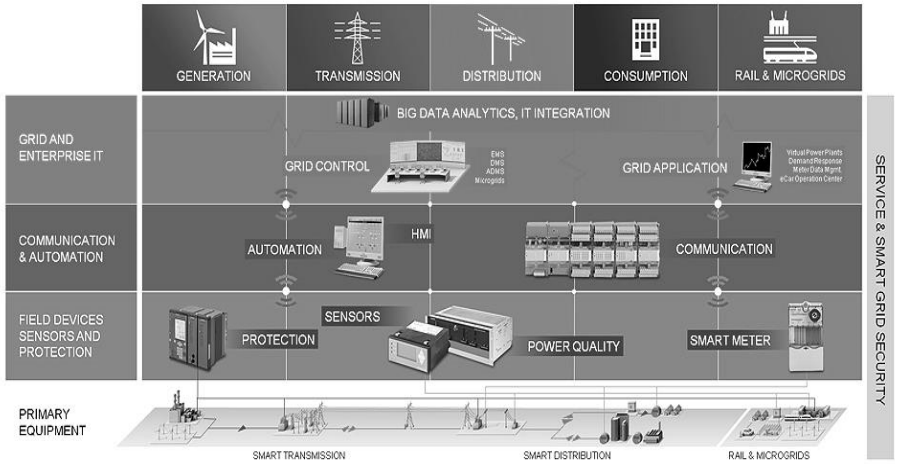

Fig. 1. Future smarter grid infrastructure technologies, adapted from [29].

Here is where the critical switch concept emerges; i.e. the ideal number of manual switches that has to be replaced with RCSs in order to optimally meet multiple objectives such as the optimal integration and use of renewable DGs in the most economical way [22]. To evaluate the performance of electrical systems, some indices such as the System Average Interruption Frequency Index (SAIFI), the System Average Interruption Duration Index (SAIDI) and the Customer Average Interruption Duration Index (CAIDI) are usually used. These indices include the so-called extended service outlets, those that last longer than five minutes. An automated system reduces the number of these service outages, locates and isolates the fault automatically and almost instantaneously, thus preventing service outages in zones that do not belong to the fault zone [11], [12], [17], [23].

Energy production in large power plants and their delivery at points of consumption constitute the classic tasks of a power grid. However, the technological advance and the evolution of the human need have raised some difficulties in terms of operation, control, efficiency and reliability, which require a change of perspective [24], including large number of components interconnected to the distribution network. Any failure of a component can easily affect another component in the system instantly. This is due to several system-wide interconnections and high interdependencies among components and networks in the system, which make the development of mathematical models a complex challenge.

Distribution network automation enhances the utility of DSR because the automation enables an optimal and speedy response to possible problems in the system. This reduces the number of interventions by the operator, and leaves the network less subject to human error [23]. However, for large-scale systems with a more complex topology, the computational load may be quite high, resulting in slow DSR decision and limiting the system restoration performance.

However, with the advance of computational tools and distributed computing, this may not be a major issue. Moreover, the evolution distribution systems to smart grids, equipped with the integration of sensor-based technologies, state-of-the-art control methods and (bidirectional) communication systems among others, is viewed as a possible solution to the challenges.

Smart girds adopt decentralized control features, which increases network flexibility and improves a host of other features such as: the utility of DSR, restoration and even fault detections, coordination of protections and voltage control [7], [24]–[28]. Fig 1 presents the key technologies and important aspects required to develop smarter grid infrastructures.

Generally, distribution system automation has been attracting a lot of attention in recent years mainly due to the increasing penetration of variable energy sources. This is part of the effort to ensure seamless integration of such resources and enhance grid reliability and system stability. Smart grids, equipped with self-healing mechanisms, can not only automatically detect faults and act accordingly but also make a quicker restoration possible. This substantially improves, the overall reliability in the considered system. The goal of self-healing is to minimize the duration of service outages as well as interruptions felt by consumers, eventually increasing the reliability of the system [9], [17], [26]–[28].

Therefore, the future of power systems is one of the hot topics where majority of roadmaps grid smartification, which has the ability to perform operations in an automated manner, with higher reliability and low operating and maintenance costs. The work in [29] summarizes ongoing research and development in the smart grid arena. Remotely controlled switches and new communication technologies play important roles in the transition to smart grids [30].

B. Literature Review

The main aim of system reconfiguration in the extant literature has mainly been to minimize network losses [31], [32]. To some extent, this is coordinated with optimal allocations of distributed generations [31], [32]. However, in recent years, DSR has been gaining more attention due to the new challenges facing power systems in general, distribution systems in particular.

From the smart grids perspective, system automation facilitates optimal use of DSR under normal operation. The utility of DSR in contingency cases is also tied with the self-healing process, a key part of the smart grid concept. Therefore, DSR is a key element which enables a more autonomous and efficient recovery from contingency to a normal operating state. From the smart grid perspective, earlier works related to DSR are limited.

This article has been accepted for publication in a future issue of this journal, but has not been fully edited. Content may change prior to final publication. Citation information: DOI 10.1109/TIA.2019.2930433, IEEE Transactions on Industry Applications

Regarding the analysis of reliability indices, Paterakis *et al.* [32] present a study on system reconfiguration formulated through a multi-objective problem and with the aim of minimizing network losses while also optimizing some reliability indices. In the same context, Chen *et al.* [33] presents a method that analyzes some reliability indices taking into account network reconfiguration and daily demand data.

Regarding switches and their central role in system reconfiguration and restoration, several papers address optimal ways to allocate switches along network systems [34], [35]. One of the most important points about switches is the replacement of manual switches with RCSs. Bernardon *et al.*, in [36], presents a new methodology for the DSR to be done automatically, incorporating DG units in the operation of the system and only considering RCSs. The problem in this method is that it is not practical to consider all switches as RCSs. This is because of the fact that replacing all manual switches may be excessively expensive or impractical.

Having this in mind, Lei *et al.* [21] introduces the concept of "critical switch", which represents the minimum number of manual switches to be replaced by RCSs that will make dynamic reconfiguration more efficient. Thus, the work in [21] studies the application of DSR with DG integration and seeks to minimize energy losses while also identifying the switches that needs to be replaced at the lowest possible cost.

Despite this, Lei *et al.* does not solve the problem of optimal allocation of RCSs. Therefore, after identifying the number and the switches that need to be replaced, the biggest problem lies on where to place the RCSs to maximize their performance. Authors in [19] have introduced new methods that allow an optimal RCS allocation so that the system's restoration performance and the overall system reliability can be improved, both at the lowest possible cost.

In [35], Ray *et al.* argue that the optimization of the number and locations of RCSs must take into account three different main objectives: the minimizations of service interruption cost, service interruption duration index (SAIDI), and maximization of the quantity of loads that can be restored using the RCSs. A model formulated as a Mixed Integer Conic Programming (MICP) is proposed that seeks to optimize the number and locations of RCSs so that automatic restoration is ensured, and this is done as fast as possible.

This paper presents a new framework to determine the minimal set of switches that have to be replaced or optimally allocated in order to automate the system. This is supported by a sensitivity analysis. Different topologies are also assessed taking into account various reliability indices and power losses in system operation following the system's automation. Such an optimization work is done under a massive integration of renewable energy sources and energy storage systems. All this simultaneously addresses the economic and functional requirements of the automated system, ultimately improving system's reliability. The standard IEEE 119-bus standard system is used as a case study, where different types of loads are considered (residential, commercial and industrial).

One of the salient features of the new approach presented in our work is its multi-sequential structure (explained in detail in the next section), where system reliability is improved in each step. This makes it unique from any of those suggested in the literature.

C. Contributions and Paper Organization

The current work is designed to perform an extensive analysis with regards to DSR in terms of improving the system's restoration capability after a contingency. For this reason, the system is dynamically reconfigured, with a goal of identifying the minimum number of switches that must be replaced with RCSs. This eventually improves the system's overall performance. Moreover, further analysis is made considering that the system has already been automated, established based on previous results. However, even if distribution systems are adequately equipped to make dynamic reconfigurations possible, it should be noted that technical and economic barriers exist that do constrain frequent reconfigurations (such as hourly). Therefore, according to the literature and the demand response models, an optimization of three different topologies (one per each load period) is preferred, following a set of criteria. To optimize the system operation, two reliability indices, SAIFI and SAIDI are used, along with system losses. Here, a TOPSIS decision support tool is subsequently used to identify the best configuration for the considered periods (each with a set of hours), where different case studies are analyzed. The flowchart in Fig. 2 shows the entire approach adopted in this work.

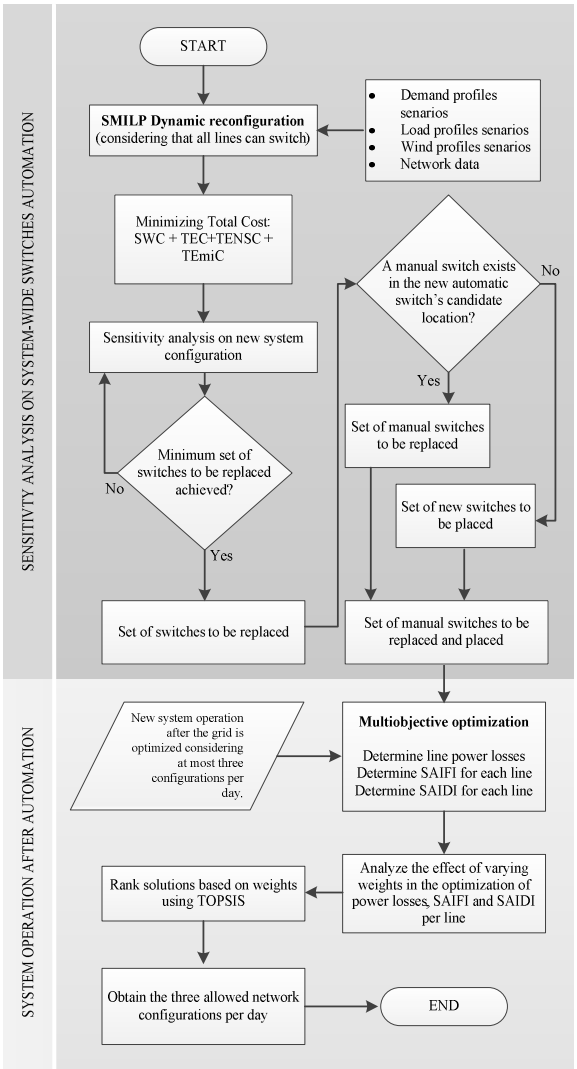

Fig. 2. A flowchart of the methodology.

This article has been accepted for publication in a future issue of this journal, but has not been fully edited. Content may change prior to final publication. Citation information: DOI 10.1109/TIA.2019.2930433, IEEE Transactions on Industry Applications

The main contributions of this paper are the following:

- An improved stochastic mixed integer linear programming (SMILP) operation model considering the presence of distributed generation-based renewables, energy storage systems and dynamic reconfiguration, where a linearized AC-OPF (Alternating Current - Optimal Power Flow) model attains the right balance between accuracy and computational complexity.
- A methodology for system-wide sensitivity analysis to identify the minimum set of switches to be updated from manual to automatic ones, determined according to an optimal dynamic reconfiguration.
- Analysis on whether the automated switches need to be placed in locations where manual switches already exist or even elsewhere on the system.
- Identification of automatic switches that require more maintenance due to frequent dynamic reconfigurations.
- The experimental analysis with regards to different topologies considering different reliability indices (System Average Interruption Duration Index – SAIDI, and System Average Interruption Frequency Index – SAIFI) and power losses.

The remainder of this work is organized as follows. Section III presents a complete description of the developed algebraic model. Case study and discussion of numerical results are provided in Section IV. Issues related to uncertainty management are presented in Section V, and the last section concludes this paper.

III. Mathematical Formulation

The problem is formulated as a stochastic MILP optimization model. The resulting model's accuracy is guaranteed because the core of the optimization framework employs a linearized AC-OPF based network model, which has the right balance between accuracy and computational requirements.

A. Objective Function

The objective of the current work is to minimize the sum of the most relevant cost terms (1); namely, the costs related to network reconfiguration (switching), operation, emissions and load shed.

$$MinTC = SWC + TEC + TENSC + TEmiC \tag{1}$$

The switching cost term (2) is incurred when a change of status in a given line occurs, that is, when it goes from 0 (open) to 1 (closed) or vice versa.

$$SWC = \sum_{l\in\Omega^l}\sum_{h\in\Omega^h} SW_l * (y^+_{l,h} + y^-_{l,h}) \tag{2}$$

where:

$$x_{k,h} - x_{k,h-1} = y^+_{k,h} - y^-_{k,h};\ y^+_{k,h} \geq 0;\ y^-_{k,h} \geq 0$$
$$x_{k,0} = 1;\ \forall k \in \Omega^1 \text{ and } x_{k,0} = 0;\ \forall k \in \Omega^0$$

The sets Ω^1 and Ω^0 refer to the normally closed feeders and tie lines, respectively. The statuses of the feeders and tie lines can change during the optimization; that is, depending on the optimal topology obtained following the dynamic network reconfiguration. The emission cost (3) is given by the sum of costs of power produced by DGs, discharged from ESS and imported from upstream grid.

$$\begin{aligned} TEC = &\sum_{s\in\Omega^s}\rho_s\sum_{h\in\Omega^h}\sum_{g\in\Omega^g} OC_g P^{DG}_{g,n,s,h} \\ &+ \sum_{s\in\Omega^s}\rho_s\sum_{h\in\Omega^h}\sum_{es\in\Omega^{es}} \lambda^{es} P^{dch}_{es,n,s,h} \\ &+ \sum_{s\in\Omega^s}\rho_s\sum_{h\in\Omega^h}\sum_{\varsigma\in\Omega^\varsigma} \lambda^{\varsigma}_h P^{SS}_{\varsigma,n,s,h} \end{aligned} \tag{3}$$

The cost of load shedding, given by *TENSC*, is formulated as follows:

$$TENSC = \sum_{s\in\Omega^s}\rho_s\sum_{h\in\Omega^h}(v^P_{s,h}P^{NS}_{n,s,h} + v^Q_{s,h}\,Q^{NS}_{n,s,h}) \tag{4}$$

Here, $v^P_{s,h}$ and $v^Q_{s,h}$ define penalty parameters for active and reactive power that is not supplied. These two parameters are each set to a sufficiently high value, which roughly quantifies the value of lost load. Note that TENSC can also be regarded as a reliability index.

Finally, equation (5) refers to the total cost of emissions as a result of power either supplied by DGs or imported from upstream.

$$\begin{aligned} TEmiC = &\sum_{s\in\Omega^s}\rho_s\sum_{h\in\Omega^h}\sum_{g\in\Omega^g}\sum_{n\in\Omega^n} \lambda^{CO_2}\,ER^{DG}_g P^{DG}_{g,n,s,h} \\ &+ \sum_{s\in\Omega^s}\rho_s\sum_{h\in\Omega^h}\sum_{\varsigma\in\Omega^\varsigma}\sum_{n\in\Omega^n} \lambda^{CO_2}\,ER^{SS}_\varsigma P^{SS}_{\varsigma,s,h} \end{aligned} \tag{5}$$

B. Constraints

The healthy operation of distribution systems is guaranteed by respecting the technical and economic constraints during all operation times. One of the major technical constraints is the Kirchhoff's current law, which states that the sum of all flows arriving at a bus must be always equal to the sum of all flows leaving that bus at any time.

The sum of all incoming flows to a node should be equal to the sum of all outgoing flows, which is given by the *Kirchhoff's Law*. This is applied to both active (6) and reactive (7) power flows, and must be respected at all times:

$$\begin{aligned} &\sum_{g\in\Omega^g} P^{DG}_{g,n,s,h} + \sum_{es\in\Omega^{es}}\left(P^{dch}_{es,n,s,h} - P^{ch}_{es,n,s,h}\right) + P^{SS}_{\varsigma,s,h} \\ &+ P^{NS}_{n,s,h} + \sum_{in,l\in\Omega^l} P_{l,s,h} - \sum_{out,l\in\Omega^l} P_{l,s,h} = PD^n_{s,h} \\ &+ \sum_{in,l\in\Omega^l}\frac{1}{2}PL_{l,s,h} + \sum_{out,l\in\Omega^l}\frac{1}{2}PL_{l,s,h};\ \forall\varsigma\in i \end{aligned} \tag{6}$$

$$\begin{aligned} &\sum_{g\in\Omega^g} Q^{DG}_{g,n,s,h} + Q^c_{c,n,s,h} + Q^{SS}_{\varsigma,s,h} + Q^{NS}_{n,s,h} \\ &+ \sum_{in,l\in\Omega^l} Q_{l,s,h} - \sum_{out,l\in\Omega^l} Q_{l,s,h} = QD^n_{s,h} \\ &+ \sum_{in,l\in\Omega^l}\frac{1}{2}QL_{l,s,h} + \sum_{out,l\in\Omega^l}\frac{1}{2}QL_{l,s,h}\ \forall\varsigma\in i \end{aligned} \tag{7}$$

Equations (8) and (9) present the linearized AC power flows through each feeder, which are governed by the *Kirchhoff's Voltage Law*. This is considered by including linearized power flow equations. Such a linearization method follows two assumptions. First, the voltage angle difference θ_k is normally very small in distribution networks. In trigonometric approximations, this results in $\sin\theta_k \approx \theta_k$ and $\cos\theta_k \approx 1$.

This article has been accepted for publication in a future issue of this journal, but has not been fully edited. Content may change prior to final publication. Citation information: DOI 10.1109/TIA.2019.2930433, IEEE Transactions on Industry Applications

Second, the bus voltage magnitudes are expected to be close to the rated value V_{nom} in distribution systems. $\Delta V_{i,s,h} - \Delta V_{j,s,h}$ is the voltage deviation between the branch input and output node for a given scenario and hour.

By using these simplifying assumptions, the complex nonlinear and nonconvex flow equations can be linearized as:

$$\begin{aligned} &\left|P_{l,s,h} - (V_{nom}\left(\Delta V_{n,s,h} - \Delta V_{m,s,h}\right)g_k \right. \\ &\left. - V_{nom}^2 b_k \theta_{l,s,h}\right| \le MP_l(1-\chi_{l,h}) \end{aligned} \tag{8}$$

$$\begin{aligned} &\left|Q_{l,s,h} - (-V_{nom}\left(\Delta V_{n,s,h} - \Delta V_{m,s,h}\right)b_k \right. \\ &\left. - V_{nom}^2 g_k \theta_{l,s,h}\right| \le MQ_l(1-\chi_{l,h}) \end{aligned} \tag{9}$$

The maximum amount of flow that can pass through a line is given by inequality (10). Equations (11) and (12) represent active and reactive power losses in a given line.

$$P_{l,s,h}^2 + Q_{l,s,h}^2 \le \chi_{l,h}(S_l^{max})^2 \tag{10}$$

$$PL_{l,s,h} = R_l\left(P_{l,s,h}^2 + Q_{l,s,h}^2\right)/V_{nom}^2 \tag{11}$$

$$QL_{l,s,h} = X_l\left(P_{l,s,h}^2 + Q_{l,s,h}^2\right)/V_{nom}^2 \tag{12}$$

An energy storage system is modeled by the expressions (13)-(18).

$$0 \le P_{es,n,s,h}^{ch} \le I_{es,n,s,h}^{ch} P_{es,n,h}^{ch,max} \tag{13}$$

$$0 \le P_{es,n,s,h}^{dch} \le I_{es,n,s,h}^{dch} P_{es,n,h}^{ch,max} \tag{14}$$

$$I_{es,n,s,h}^{ch} + I_{es,n,s,h}^{ch} \le 1 \tag{15}$$

$$E_{es,n,s,h} = E_{es,n,s,h-1} + \eta_{es}^{ch} P_{es,n,s,h}^{cg} - \frac{P_{es,n,s,h}^{dch}}{\eta_{es}^{dch}} \tag{16}$$

$$E_{es,n}^{min} \le E_{es,n,s,h} \le E_{es,n}^{max} \tag{17}$$

$$E_{es,n,s,h0} = \mu_{es} E_{es,n}^{max};\ E_{es,n,s,h24} = \mu_{es} E_{es,n}^{max} \tag{18}$$

The limits on the amount of power charged and discharged are given by (13) and (14), respectively, while (15) guarantees that charging and discharging processes do not simultaneously happen at any given time.

The state of charge is modelled as presented in (16). Inequality (17) ensures that the storage level is always within a permissible range. Finally, (18) sets the initial storage level, and ensures the storage is left with the same amount at the end of the operational period.

The active and reactive power limits of DGs are given by (19) and (20), respectively.

Inequality (21) limits the DGs ability to inject or consume reactive power.

$$P_{g,n,s,h}^{DG,min} \le P_{g,n,s,h}^{DG} \le P_{g,n,s,h}^{DG,max} \tag{19}$$

$$Q_{g,n,s,h}^{DG,min} \le Q_{g,n,s,h}^{DG} \le Q_{g,n,s,h}^{DG,max} \tag{20}$$

$$\begin{aligned} -\tan\left(cos^{-1}(pf_g)\right)P_{g,n,s,h}^{DG} &\le Q_{g,n,s,h}^{DG} \\ &\le tan\left(cos^{-1}(pf_g)\right)P_{g,n,s,h}^{DG} \end{aligned} \tag{21}$$

However, it should be noted that these constraints are applicable only for conventional DGs which have reactive power support capabilities. In the case of variable generation sources, slight modifications are required. For instance, for wind and solar PV generators, the upper bound $P_{g,i,s,h}^{max}$ should be equal to the actual production level at a specific hour, which in turn depends on the level of primary energy source (wind speed and solar radiation). The lower bound $P_{g,i,s,h}^{min}$ in this case is simply set to zero. In addition, conventional wind and solar PV sources do not often have the capability to provide reactive power support; hence, they are operated at a constant and lagging or unity power factor.

The active and reactive power limits at each substation are given by (22) and (23), due to stability reasons.

$$P_{ç,s,h}^{SS,min} \le P_{ç,s,h}^{SS} \le P_{ç,s,h}^{SS,max} \tag{22}$$

$$Q_{ç,s,h}^{SS,min} \le Q_{ç,s,h}^{SS} \le Q_{ç,s,h}^{SS,max} \tag{23}$$

The reactive power that is withdrawn from the substation and DGs is subject to the bounds presented in inequality (24).

$$\begin{aligned} -\tan\left(cos^{-1}(pf_{ss})\right)P_{ç,s,h}^{SS} &\le Q_{ç,s,h}^{SS} \\ &\le tan\left(cos^{-1}(pf_{ss})\right)P_{ç,s,h}^{SS} \\ -\tan\left(cos^{-1}(pf_g)\right)P_{g,s,h}^{SS} &\le Q_{g,s,h}^{SS} \\ &\le tan\left(cos^{-1}(pf_g)\right)P_{g,s,h}^{SS} \end{aligned} \tag{24}$$

The above two inequalities show that wind and solar type DGs are capable of operating between pf_g leading power factor (capacitive) and pf_g lagging power factor (reactive). This means such DGs are capable of "producing" and "consuming" reactive power depending on operational situations in the system. The radial operation of the considered system is guaranteed by including the constraints in (25) through (31). Constraints (27)—(31) ensure radiality in the presence of DGs, and simultaneously avoid islanding.

$$\sum_{l\in\Omega^l} \chi_{l,h} = 1, \forall m \in \Omega^D; l \in n \tag{25}$$

$$\sum_{in,l\in\Omega^l} \chi_{l,h} - \sum_{out,l\in\Omega^l} \chi_{l,h} \le 1, \forall m \notin \Omega^D; l \in n \tag{26}$$

$$\sum_{in,l\in\Omega^l} f_{l,h} - \sum_{out,l\in\Omega^l} f_{l,h} = g_{n,h}^{SS} - d_{n,h}, \forall n \in \Omega^ç; l \in n \tag{27}$$

$$\sum_{in,l\in\Omega^l} f_{l,h} - \sum_{out,l\in\Omega^l} f_{l,h} = -1, \forall n \in \Omega^g; \forall n \in \Omega^D \tag{28}$$

$$\sum_{in,l\in\Omega^l} f_{l,h} - \sum_{out,l\in\Omega^l} f_{l,h} = 0, \forall n \notin \Omega^g; \forall n \notin \Omega^D \forall n \notin \Omega^ç \tag{29}$$

$$0 \le \sum_{in,l\in\Omega^l} f_{l,h} + \sum_{out,l\in\Omega^l} f_{l,h} \le n_{DG}; l \in n \tag{30}$$

$$0 \le g_{n,h}^{SS} \le n_{DG}, \forall n \in \Omega^ç; l \in n \tag{31}$$

C. Reliability Indices

In this work, some reliability indices are used after the optimization processes to support the decision-making with regards to the system's optimal operation. The reliability indices taken into account are the System Average Interruption Frequency Index (SAIFI) and System Average Interruption Duration Index (SAIDI), which are calculated using equations (32) and (33).

SAIFI is given by the total number of consumer's interruption duration by the total number of consumers; however, this study focuses on the impact of branch failures to the customers served, such as the reformulated index in (32).

$$SAIFI = \left(\frac{\sum_{l\epsilon\Omega} l \quad \lambda_l * |cf_l|}{M}\right) x_{l,h} \tag{32}$$

In the above equation, λ_l is the rate of failure that affects N_n customers; $|cf_l|$ is the number of clients supplied by line l and M is the total number of customers. SAIFI is calculated for each line and for each hour. $x_{l,h}$ refers to the status of each line, whose value is zero if the line is not connected; otherwise, it is set to 1.

SAIDI is given by the total number of consumer's interruption duration by the total number of consumers. In this study, this is calculated as a weighted mean of the duration of the interruptions assuming the number of customers as weights (33).

This article has been accepted for publication in a future issue of this journal, but has not been fully edited. Content may change prior to final publication. Citation information: DOI 10.1109/TIA.2019.2930433, IEEE Transactions on Industry Applications

$$SAIDI = \left(\frac{\sum_{l\epsilon\Omega} l \quad \lambda_l * U_l * |cf_l|}{M}\right) x_{l,h} \tag{33}$$

In this equation, U_l is the average repair time of line l. SAIDI is also calculated for each line and each hour. Note that $x_{l,h}$ is zero if a given line is not connected ($x_{l,h} = 0$).

D. Technique for Order of Preference by Similarity to Ideal Solution (TOPSIS) Formulation

This work employs the TOPSIS technique as a decision analysis tool. Its algebraic representation is given by Eqs. (34) – (41).

TOPSIS is a multi-criteria decision analysis method which is used to generate a Pareto front by evaluating *p*-objectives in a decision matrix. The TOPSIS method evaluates the following decision matrix (DM):

$$DM = \begin{bmatrix} x_{1,1} & \cdots & x_{1,m} & \cdots & x_{1,p} \\ \vdots jj & \ddots j & \vdots jj & \ddots j & \vdots jj \\ x_{n,1} & \cdots & x_{n,m} & \cdots & x_{p,m} \\ \vdots jj & \ddots j & \vdots jj & \ddots j & \vdots jj \\ x_{r,1} & \cdots & x_{r,m} & \cdots & x_{r,p} \end{bmatrix} \tag{34}$$

where m are the possible alternatives and n refer to the criteria. $X_{i,j}$ represents the rating and performance of alternative n subject to criterion m. Each line of (34) represents an alternative solution, while each column is associated with an objective function (which can be minimization or maximization). In the general case, each objective is expressed in different units. Thus, the next step of the TOPSIS method is to transform the decision matrix into a non-dimensional attribute matrix in order to enable a comparison among the attributes. The normalization process is performed through the division of each element by the norm of the vector (column) of each criterion.

An element $f_{n,m}$ of the normalized matrix is given by (35):

$$f_{n,m} = \frac{x_{n,m}}{\sqrt{\sum_{K=1}^{p} x_{km}^2}} \tag{35}$$

A set of weights as in (36), which express the relative importance of each objective (criterion), is provided by the Decision Maker at this point. The weighted normalized matrix with elements is created by multiplying each column of the matrix with elements by the weight.

$$w = \{w_1, \dots, w_{1m}, \dots w_p, \}, \sum_{m}^{n} w_m = 1 \tag{36}$$

The next step is to specify the ideal and the negative-ideal solution vectors. In (37) and (38), Ma is the set of objectives (criteria) to be maximized and Ma' is the set of objectives to be minimized. These artificial alternatives indicate the most preferable (ideal) solution and the least preferable (negative-ideal) solutions.

$$A^+ = \{(max_n(e_{n,m})|m \in Ma), (min_n(e_{n,m})|m \in Ma')\}, \forall n = 1, \dots, m \tag{37}$$

$$A^- = \{(min_n(e_{n,m})|m \in Ma), (max_n(e_{n,m})|m \in Ma')\} \forall n = 1, \dots, m \tag{38}$$

Then, the separation measure of each alternative from the ideal and the negative-ideal solution is measured by the dimensional Euclidean distance (39) and (40):

$$S_n^+ = \sqrt{\sum_{m=1}^{n} \left(e_{n,m} - e_m^+\right)^2}, \forall n = 1, \dots, m \tag{39}$$

$$S_n^- = \sqrt{\sum_{m=1}^{n} \left(e_{n,m} - e_m^-\right)^2}, \forall n = 1, \dots, m \tag{40}$$

The final step in the application of the TOPSIS method is the calculation of the relative closeness to the ideal solution. In (41), these distances are computed in order to create a rank (from the highest to the lowest value) of hourly topologies.

$$C_n^+ = \frac{S_n^-}{S_n^+ + S_n^-}, \quad 0 < C_n^+ < 1, \forall n, \dots, m \tag{41}$$

IV. Uncertainty and Variability Management

Supply-side variability and uncertainty are non-exclusive characteristics of renewable power generation. There are other parameters in the optimization process that are also characterized by these variables. In this work, three sources of uncertainty and variability are identified, namely wind, solar and demand.

To account for demand uncertainties, two demand profile scenarios are taken, considering a ±5% prediction error margin from real-life short-term demand profile (i.e. 24 hours). This then leads to three demand scenarios, which are used in the analysis. Wind speed and solar radiation are generated following the methodology in [37]. The average wind speed and solar radiation profiles are obtained based on real data. These values are plugged in equations (42) and (43) to obtain the respective power outputs. The power outputs cannot be used straightforward because they may not directly maintain the proper correlation with the average demand profile. Therefore, the power outputs should be readjusted to replicate the time-based correlations that happen between demand, solar radiation and wind speed. The correlation between wind and solar, wind and demand, and solar and demand are respectively -0.3, 0.28, 0.5, being obtained from [37].

After obtaining the correlation matrix, the wind and solar power outputs can be transformed into new ones, given the correlation between them. Cholesky factorization is used to adjust the data series. The method consists of having a correlation matrix R, uncorrelated data D, so that a new data C, whose correlation matrix is R, is generated by multiplying the Cholesky decomposition of R by D. The power output profiles are determined by using these readjusted values. Note that the following power curve is used in converting the wind speed into power:

$$P_{wind,h} = \begin{cases} 0; & 0 \le v_h \le v_{ci} \\ P_r\left(A + Bv_h^3\right); & v_{ci} \le v_h \le v_r \\ P_r; & v_r \le v_h \le v_{co} \\ 0; & v_h \ge v_{co} \end{cases} \tag{42}$$

In eq. (43), parameters A and B are given by the expressions in [37]. In the same way, the solar power output are determined using the following expression:

$$P_{solar,h} = \begin{cases} \frac{P_r R_h^2}{R_{std} R_c}; & 0 \le R_h \le R_c \\ \frac{P_r R_h}{P_{std}}; & v_{ci} \le R_h \le std \\ P_r; & R_h \le R_{std} \end{cases} \tag{43}$$

This article has been accepted for publication in a future issue of this journal, but has not been fully edited. Content may change prior to final publication. Citation information: DOI 10.1109/TIA.2019.2930433, IEEE Transactions on Industry Applications

Uncertainty pertaining to wind and solar power productions is assumed to have ±15% deviation from the average power output profiles. This translates approximately to a ±5% forecasting error in wind speed or solar radiation, in line with the best existing forecasting tools present in the market [38]-[41]. The hourly profiles of wind and solar power outputs are constructed based on the considered deviations. This is transformed into three wind and solar power outputs profiles (namely, high, low and average). The individual scenarios of demand, wind and solar power outputs are combined to form a set of 27 scenarios (i.e. 3*3*3). All of these scenarios are assumed to be equally probable; hence, with ρ_s equal to 1/27.

V. Numerical Results

A. Data and Assumptions

The standard IEE 119-bus test system is used as a case study. Fig. 3 shows its schematic diagram, and the locations and types of distributed energy resources in the system. The placement and sizing of DGs and ESSs are based on [43]. Detailed data about this test system can be found in [42]. The notations of feeders in the considered system are presented in Appendix A. In this system, there are two types of DGs, solar and wind which have an installed capacity of 2 MW and 1 MW, respectively. The ESSs have as installed capacity of 1 MW with both charging and discharging efficiencies assumed to be 90%. The operational period is assumed to be 24 hours long. A possible hourly reconfiguration is considered. The voltage level of the system is 10 kV, and the maximum voltage deviation allowed at each node is ± 5% of the nominal value. The substation is considered as the reference node, where voltage magnitude deviation and angle are both set to 0.

In addition, the power factor at the substation is set to 0.95, and is kept constant throughout. Electricity prices follow the demand trend, ranging from 42 to 107 €/MWh. The lowest electricity price happens during the valley periods and the highest ones during peak consumption periods. The operation cost of ESSs during charging and discharging is considered to be 5 €/MWh. The rate of emissions at the substation is assumed to be 0.4 tCO2e/MWh, and a carbon price of 7 €/tCO2 is considered in all simulations. A tariff of 40 €/MWh and 20 €/MWh are considered for remunerating the power productions from solar PV and wind farms. The cost of switching any line is considered to be 5 €/switching.

B. Analysis on Dynamic Reconfiguration and System Restoration Capability

In this work, the possibility of automating switches is considered via dynamic network reconfiguration in the presence of renewables (wind and solar) and ESSs. The reconfiguration involves multiple phases. The aim of such a reconfiguration is to find the best topology that optimizes system operation in a given period while fulfilling economic requirements and technical restrictions. Table I shows the cost terms and losses in the system. A key observation in this table is that the integration of smart grid enabling technologies minimizes chances of involuntary load shedding (which is zero in current study). The presence of DGs combined with ESSs leads to all demand being met while the stability and reliability of the system are maintained at the required levels.

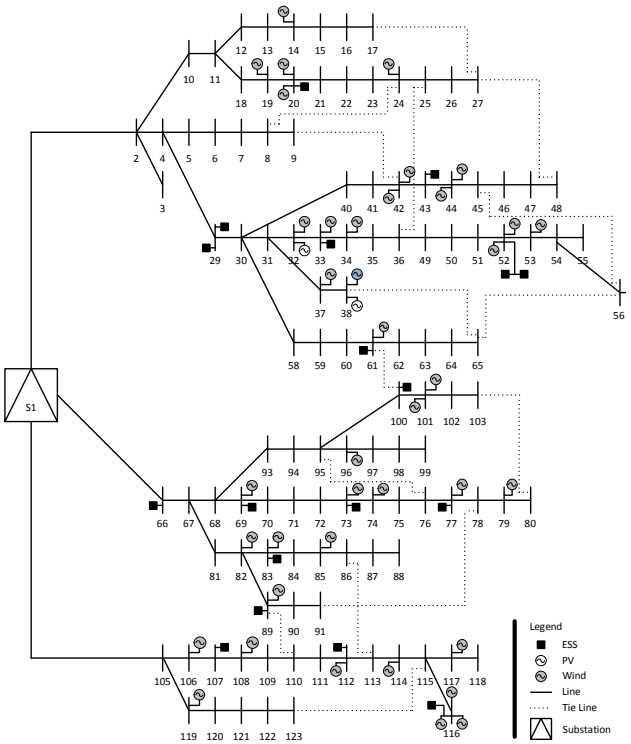

Fig. 3. The IEEE standard 119 Bus test system.

TABLE I – System Costs [43]

Total Cost [€]	29912,27
Reconfiguration Cost [€]	1010,00
Energy Cost [€]	27901,72
Emission Cost [€]	1000,55
Power nor served [€]	0,00
Active Power Losses [MW/day]	10,00
Reactive Power Losses [MVAr/day]	6,60

Table I also reveals a substantial reduction of energy losses as a result of the dynamic reconfiguration and joint integration of DGs and ESSs. In the absence of these measures, losses would otherwise be considerably higher [43]. The reconfiguration results are presented in Table II, where the set of closed and open lines constitute the optimal network topology in each time period.

In the first phase, a system-wide dynamic reconfiguration has been carried out, and hourly reconfigurations are obtained. The reconfiguration outcomes can be found in [44], where the set of closed and open lines constitute an optimal topology.

In the second phase, a sensitivity analysis is further performed to complement the outcome of the dynamic reconfiguration results obtained in the first phase. Based on the analysis of dynamic reconfiguration, the number of switching operations per line is analyzed. The analysis results are depicted in Fig. 4.

It should be noted that the dynamic reconfiguration in the previous phase is carried out under the assumption that all lines can be reconfigured. However, in reality, there can be restrictions or conditions that inhibit switching certain lines. If such lines are known from the outset, they can be excluded from the reconfiguration pool, which simplifies the analysis and the problem to be solved. To do this, one simply needs to define a new set of lines that can be switched. The model and the methodology remains valid regardless.

This article has been accepted for publication in a future issue of this journal, but has not been fully edited. Content may change prior to final publication. Citation information: DOI 10.1109/TIA.2019.2930433, IEEE Transactions on Industry Applications

TABLE II –NETWORK RECONFIGURATION FOR EACH HOUR (WITHIN A 24 HOURS PERIOD) [39]

Hour	Closed Lines	Open Lines
1	1-22; 24; 25; 27-33; 35-60; 62-81; 83-89; 91-94; 96-116; 118; 120; 123; 125; 126; 129; 131; 132;	23; 26; 34; 61; 82; 90; 95; 117; 119; 121; 122; 124; 127; 128; 130;
2	1-22; 24; 25; 27-33; 35-41; 43-60; 62-75; 77-81; 83; 84; 86-89; 91-94; 96-118; 120; 121; 123; 125; 126; 128-130; 132;	23; 26; 34; 42; 61; 76; 82; 85; 90; 95; 119; 122; 124; 127; 131;
3	1-22; 24; 25; 27-33; 35-60; 62-73; 75; 77-81; 83; 84; 86-89; 91-94; 96-118; 120; 123; 125-130; 132;	23; 26; 34; 61; 74; 76; 82; 85; 90; 95; 119; 121; 122; 124; 131;
4	1-22; 24; 25; 27-33; 35-52; 54-60; 62-73; 75; 77-81; 83; 84; 86-89; 91-94; 96-117; 119; 120; 122; 123; 125-130; 132;	23; 26; 34; 53; 61; 74; 76; 82; 85; 90; 95; 118; 121; 124; 131;
5	1-22; 24; 25; 27-33; 35-41; 43-52; 54-60; 62-73; 75; 77-81; 83-89; 91-94; 96-117; 119-123; 125-129; 132;	23; 26; 34; 42; 53; 61; 74; 76; 82; 90; 95; 118; 124; 130; 131;
6	1-22; 24; 25; 27-33; 35-52; 54-60; 62-73; 75; 77-81; 83-89; 91-94; 96-117; 119; 120; 122; 123; 125-129; 132;	23; 26; 34; 53; 61; 74; 76; 82; 90; 95; 118; 121; 124; 130; 131;
7	1-22; 24; 25; 27-33; 35-41; 43-60; 62-73; 75; 77-89; 91-94; 96-118; 120; 121; 123; 125-128; 132;	23; 26; 34; 42; 61; 74; 76; 90; 95; 119; 122; 124; 129-131;
8	1-22; 24; 25; 27-33; 35-52; 54-60; 62-81; 83; 84; 86-89; 91-94; 96-118; 120; 122; 123; 125; 126; 129; 130; 132;	23; 26; 34; 53; 61; 82; 85; 90; 95; 119; 121; 124; 127; 128; 131;
9	1-22; 24; 25; 27-33; 35-60; 62-81; 83; 84; 86-89; 91-94; 96-118; 120; 123; 125; 129; 130; 132;	23; 26; 34; 61; 82; 85; 90; 95; 119; 121; 122; 124; 126-128; 131;
10	1-22; 24; 25; 27-33; 35-38; 40-52; 54-60; 62-89; 91-94; 96-118; 120; 122; 123-126; 132;	23; 26; 34; 39; 53; 61; 90; 95; 119; 121; 127-130; 131;
11	1-22; 24; 25; 27-33; 35-38; 40-52; 54-60; 62-73; 75-117; 119; 120; 122-124; 126; 127; 132;	23; 26; 34; 39; 53; 61; 74; 118; 121; 125; 128-130; 131;
12	1-22; 24; 25; 27-33; 35-38; 40-60; 62-84; 86-89; 91-118; 120; 123; 124; 130; 132;	23; 26; 34; 39; 61; 85; 90; 119; 121; 122; 125; 116-129; 131;
13	1-22; 24; 25; 27-33; 35-52; 54-60; 62-89; 91-94; 96-118; 120; 122; 123; 125; 126; 132;	23; 26; 34; 53; 61; 90; 95; 119; 121; 124; 127; 128-130; 131;
14	1-22; 24; 25; 27-33; 35-60; 62-73; 75-81; 83;84; 86-117; 120; 123; 127; 129; 130; 132;	23; 34; 61; 74; 82; 85; 118; 119; 121; 122; 124-126; 131;
15	1-22; 24; 25; 27-33; 35-60; 62-73; 75-81; 83; 84; 86-116; 120; 123; 127; 129-132;	23; 34; 61; 74; 82; 85; 117-119; 124-126; 128;
16	1-22; 24; 25; 27-33; 35-38; 40-52; 54-60; 62-84; 86-117; 120; 122-124; 130; 132;	23; 34; 39; 53; 61; 85; 118; 119; 121; 125-129; 131;
17	1-22; 24; 25; 27-33; 35-52; 54-60; 62-73; 75-89; 91-94; 96-116; 119; 120; 122; 123; 125-127; 131; 132;	23; 26; 34; 53; 61; 74; 90; 95; 117; 118; 121; 124; 128-130;
18	1-22; 24; 25; 27-33; 35-52; 54-60; 62-73; 74-89; 91-94; 96-118; 120; 122; 123; 125; 126; 132;	23; 26; 34; 53; 61; 90; 95; 119; 121; 124; 127-131;
19	1-25; 27-33; 35-38; 40-52; 62-84; 86-117; 119; 122; 123; 124; 130; 132;	26; 34; 39; 53; 61; 85; 118; 120; 121; 125; 126-128; 129; 131;
20	1-25; 27-33; 35-38; 40-60; 62-73; 75-118; 123; 124; 127; 132;	26; 34; 39; 61; 74; 119-122; 125; 126; 128-130;131;
21	1-25; 27-38; 40-60; 62-73; 75-84; 86-117; 86-117; 119; 123; 124; 127; 130;	26; 39; 61; 74; 85; 118; 120-122; 125; 126; 128; 129; 131; 132;
22	1-22; 24-33; 35-38; 40-52; 54-60; 62-75; 77-81; 83; 84; 86-117; 120; 122-124; 128-130; 132;	23; 34; 39; 53; 61; 76; 82; 85; 118; 119; 121; 125-127; 131;
23	1-22; 24; 25; 27-33; 35-52; 54-60; 62-73; 75-81; 83; 84; 86-118; 120; 122; 123; 127; 129; 130; 132;	23; 26; 34; 53; 61; 74; 82; 85; 119; 121; 124-126; 131;
24	1-22; 24; 25; 27-33; 35-41; 43-52; 54-73; 75-81; 83; 84; 86-89; 91-94; 96-116; 118; 120-122; 125-127; 129-132;	23; 26; 34; 42; 53; 74; 82; 85; 90; 95; 117; 119; 123; 124; 128;

In Figure 4, we can see that not all lines undergo reconfigurations. In fact, only 22% of the lines switch their statuses at least once during the operation horizon. This effectively means 78% of the lines do not need to be automated.

Nonetheless, the 22% of lines need not all be automated due to economic reasons. Hence, it is necessary to identify the most critical set of switches that should to be automated. To do this, we employ several criteria.

In this work, the minimum set of switches to be automated is the one that allows the realization of more than 50% of the obtained topologies (in our case, the topologies presented in Table III). As a result, the criterion of the average value is used [44].

The lines which see switching operations above the average are possible candidates for automation. Fig. 4 represents the number of switching operations per line during the considered operational period. The average number of switching is 6.3.

As previously mentioned, the number of lines to be automated depends on whether or not the number of line switching operations exceeds the average i.e. 6.3. Accordingly, Table III indicates the set of lines that needs to be automated. As we can see, this set contains lines with and without existing manual switches. Those with no existing manual switches are {*line42, line53, line74, line85, line90*}, and those with already existing manual switches are {*line118, line119, line121, line122, line126, line127 and line130*}. Note that the minimum set of switches for automation is achieved when 50% or more configurations is reached (which in this is 63%).

Another aspect considered in this analysis is quantifying the degree of maintenance of the automated switches. Since not all switches operate with the same frequency, their maintenance will vary depending on how often they act to change the network topology. Thus, logically, it will be paid more attention to those switches that act more frequently in the reconfiguration of the system. In other words, the number of switching operations of a given switch is closely correlated with the level of maintenance required. Fig. 5 shows the percentage of switching of each line which houses an automated switch. In this figure, one can infer that some switches would requires more maintenance works than others.

C. *Real-time Operation and Reliability Analysis*

In the previous section of this work, we have presented a sensitivity analysis of switches automation based on active reconfiguration. This section presents an analysis with regards to the system's operation in an automated environment.

Even if the system is adequately equipped to make dynamic reconfiguration possible, it is acknowledged that technical and economic barriers exist that may not allow frequent reconfiguration (such as hourly). Therefore, according to existing literature and demand response models, an optimization of three different topologies (one per each load period) is chosen following a set of criteria. To optimize system operation, two reliability indices, SAIFI and SAIDI are used, along with system losses. Here, a TOPSIS decision support tool is subsequently used to identify the best configurations for the considered periods (each with a set of hours), where different case studies are analyzed.

Thus, the system's reliability analysis is performed based on reliability indices and the minimization of power losses. These two objectives are related even if this is not expressed explicitly. Such a relation is, however, indirectly captured through the system operational performance. A poor system performance (which is equivalent to saying a system with unfavorable reliability indices) can result in a hefty penalty for the electricity company which is responsible to oversee the system.

This article has been accepted for publication in a future issue of this journal, but has not been fully edited. Content may change prior to final publication. Citation information: DOI 10.1109/TIA.2019.2930433, IEEE Transactions on Industry Applications

Hence, a reduction of power losses leads to a substantial improvements in the system from the economic point of view. This is the case because the energy generated to supply end-users is equal to the power supplied plus the network power losses. Generally, lower network losses lead to better economic performance in the system, and hence, more favorable reliability indices.

Using the expression in (32), the SAIFI (the total number of consumer interruption duration by the total number of consumers) is calculated as a weighted mean of the duration of the interruptions assuming the number of customers as weights.

Fig. 6 shows the hourly SAIFI and the corresponding average values. In this figure, the hourly values of a given day correspond to the sum of the SAIFI values obtained for each of the lines in the respective hour and the evolution of this index.

According to Fig. 6, the SAIFI index's average value is 0.165. The values for the frequency of interruptions varies between 0.162 and 0.17, which is considered low in real-time operational standards.

Using the expression in (33), the SAIDI (the total number of consumer interruption duration by the total number of consumers) is calculated as a weighted mean of the duration of the interruptions assuming the number of customers as weights.

Fig. 6 presents the evolution of the SAIDI index whose values are computed as the sum of the SAIDI values obtained for each line in the respective hour. The hours during in which more interruptions occur also coincide with those hours in which interruptions last longer. From the results in Fig. 6, it can be seen that the SAIDI index has an average value of approximately 0.201 and the value for the duration of the interruptions ranges between about 0.192 and 0.211.

In this work, in addition to the aforementioned indices, we have also taken into account power losses. Fig. 7 presents the hourly profile of losses, which represent the sum of all losses in the system. Closely analyzing the results in Fig. 7, one can observe the hours of the day with higher power losses; particularly, the hours 8, 9, 14, 15, 16, 22, 23 and 24. The range of power losses is found out to be between about 0.29 and 0.6 MWh. The average value is approximately 0.41 MWh.

D. Utility of the Multi-Objective Optimization

The first phase of the work assumes the possibility of changing the network topology in an hourly basis during a given operational period (e.g. a day). However, such switching a frequency may be impractical and unrealistic given the scale of changes that would be required to make an hourly reconfiguration exercise happen on a regular basis.

From this context, we have identified three reconfiguration periods, each characterized by the level of energy demand:

- Off-peak period- hours 1:00 to 7:00;
- Peak period- hours 11:00 to 13:00 and 20:00 to 22:00;
- Shoulder period- hours 8:00 to 10:00, 14:00 to 19:00, 23:00 and 24:00.

Given all this, the optimal network topology for each of these periods should in principle be different from that of any

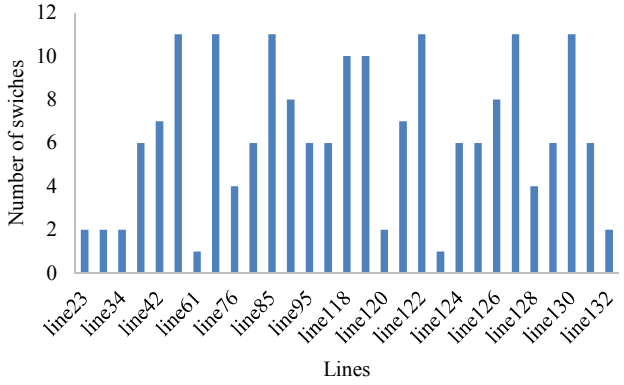

Fig. 4. Number of switching operations per line [40].

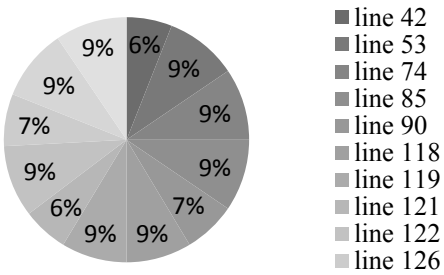

Fig. 5. Percentage of number of switching operations per line.

TABLE III –SET OF LINES FOR POSSIBLE AUTOMATION

Set of Lines to Automate
$\{line42, line53, line74, line85, line90, line118, line119, line121, line122, line126, line127, line130\}$

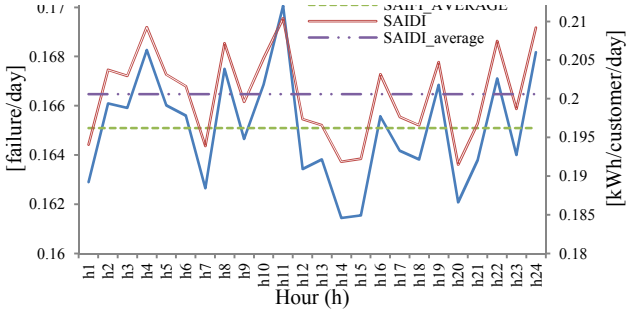

Fig. 6. Hourly SAIFI and SAIDI values and their corresponding average values in a 24-hours operation.

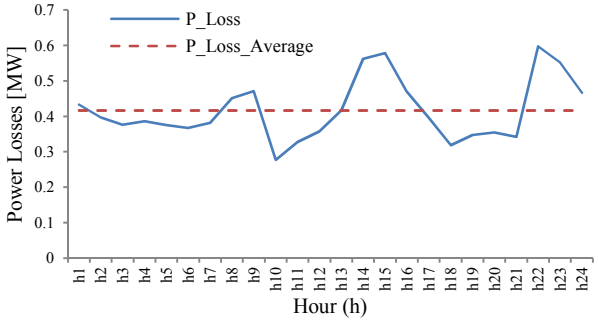

Fig. 7. Active power losses in a 24-hours operation.

This article has been accepted for publication in a future issue of this journal, but has not been fully edited. Content may change prior to final publication. Citation information: DOI 10.1109/TIA.2019.2930433, IEEE Transactions on Industry Applications

other period. This effectively means that at most three reconfigurations are performed per day. The choice of the best topology for each period is done based on the optimization of the aforementioned reliability indices and losses in a multi-objective framework.

However, it is technically impossible to optimize the three indices at the same time. This is due to the fact that optimizing one of them may result in deterioration of others. Consequently, it is necessary to find the optimum balance of all indices and power losses. For this purpose, the TOPSIS method (already presented in Section III) has been adopted in this work.

Through a multi-objective optimization, a classification of all topologies has been achieved. These are sorted out by hour and ordered from the hour with the best topology to the hour with the worst topology. And, this is always done based on the optimization of the reliability indices and losses. It is following this classification that the topology to be assumed is chosen for each one of the above periods. However, in the optimization process, the terms in the objective function do not always have the same weights. Sometimes, there is a main objective, and others are treated as secondary objectives.

From this perspective, five cases are created, and characterized by different weights given to each index in a multi-objective optimization framework. The results are shown in Table IV. The values attributed to the weights in each case allow us to study the tradeoff among the set of objectives. With these cases, it is intended that the results show the hours in which a given topology should be adopted. These results are summarized in Table V.

In the first case, the same weight has been attributed to the three indices considered in our study, in an attempt to perceive the one that will have the greatest influence on the final result.

In case 2, a higher weight has been assigned to the power losses index. As it can be seen, when a higher emphasis (weight) is given to energy losses, the ideal topology per period changes completely.

In case 3, the SAIFI index has been instead given a higher weight, which means the frequency of switching operations is given a higher priority. In this particular case, the optimal topologies for the off-peak and peak periods are found out to be similar to those obtained in case 1. On the other hand, in the shoulder period, the ideal topology again changes.

In case 4, the SAIDI index is given a higher weight, thus giving more importance to the duration of the interruptions. In this case, the optimal topology for each period is exactly the same as the ones obtained in case 3.

In case 5, higher weights are assigned to the two SAIFI and SAIDI indices, and the results obtained are exactly the same as that of case 3 and 4.

As previously mentioned, for all cases, the TOPSIS method is applied in order to identify the best network topology for each of the considered periods. In general, based on the analysis results in this work, we have not observed any clear tendency in any of the considered cases. The only exception here is perhaps when more emphasis (weight) is given to losses, which leads to dramatic changes in the reconfigurations across the time periods.

TABLE IV – ANALYSIS OF WEIGHTS FOR RELIABILITY OPTIMIZATION

Case	Weight		
	SAIFI	SAIDI	P_Loss
1	0,1	0,1	0,1
2	0,1	0,1	0,5
3	0,5	0,1	0,1
4	0,1	0,5	0,1
5	0,5	0,5	0,1

TABLE V – MULTI-OBJECTIVE OPTIMIZATION RESULTS

Period	Off-peak	Shoulder	Peak
Case 1	Hour 1	Hour 18	Hour 20
Case 2	Hour 6	Hour 10	Hour 21
Case 3	Hour 1	Hour 14	Hour 20
Case 4	Hour 1	Hour 14	Hour 20
Case 5	Hour 1	Hour 14	Hour 20

VI. CONCLUSIONS

This paper has presented an extensive analysis on the dynamic reconfiguration in conjunction with DGs and ESSs. This has been carried out from the context of operating such a system in a more reliable manner while integrating higher levels of variable RESs. To perform the analysis, an improved stochastic MILP has been employed, and a standard 119-bust test system has been used as a case study. The impact of simultaneous integration of DSR, DGs and ESSs on system's operational performance is quantified using various metrics.

The analysis results can be generally summarized as follows:

- From the dynamic reconfiguration point of view, with one or several criteria, it has been possible to jointly identify the minimum set of switches that must be automated so as not to lose the benefits of dynamic reconfiguration. Instead, system reliability is enhanced via a faster means of system restoration due to the placement of automated switches.
- The analysis also shows that the optimal locations of automated switches need not always coincide with those of existing manual switches. Moreover, the approach is able to identify the set of switches which possibly require more maintenance compared to others.

To obtain optimal reconfigurations in each period, the TOPSIS decision support tool has been used in this work. In this regard, the results generally reveal that the approach leads to a set of optimal network configurations for the three considered periods during a day in the study. These correspond to the best configurations from the perspectives of system reliability and losses. This work has also paid attention to the analysis concerning the impact of varying weights on the reliability indices and power losses, in a multi-objective optimization framework. One conclusion in this regard is that the set of configurations depends on the weight assigned for each of the objective functions considered, according to the preferences of the decision maker. However, it has been observed that losses are more sensitive to weight variations than any other reliability metric. Hence, it can be concluded that losses have the highest influence on the optimal reconfiguration outcome for each period. However, this may be case dependent.

This article has been accepted for publication in a future issue of this journal, but has not been fully edited. Content may change prior to final publication. Citation information: DOI 10.1109/TIA.2019.2930433, IEEE Transactions on Industry Applications

APPENDIX A

TABLE A.1 - NETWORK LINES

Line ID	From	To	Line	From	To	Line ID	From	To
line1	1	2	line45	47	48	line89	93	94
line2	2	3	line46	36	49	line90	94	95
line3	2	4	line47	49	50	line91	95	96
line4	4	5	line48	50	51	line92	96	97
line5	5	6	line49	51	52	line93	97	98
line6	6	7	line50	52	53	line94	98	99
line7	7	8	line51	53	54	line95	95	100
line8	8	9	line52	54	55	line96	100	101
line9	2	10	line53	54	56	line97	101	102
line10	10	11	line54	30	58	line98	102	103
line11	11	12	line55	58	59	line99	1	105
line12	12	13	line56	59	60	line100	105	106
line13	13	14	line57	60	61	line101	106	107
line14	14	15	line58	61	62	line102	107	108
line15	15	16	line59	62	63	line103	108	109
line16	16	17	line60	63	64	line104	109	110
line17	11	18	line61	64	65	line105	110	111
line18	18	19	line62	1	66	line106	111	112
line19	19	20	line63	66	67	line107	112	113
line20	20	21	line64	67	68	line108	113	114
line21	21	22	line65	68	69	line109	114	115
line22	22	23	line66	69	70	line110	115	116
line23	23	24	line67	70	71	line111	115	117
line24	24	25	line68	71	72	line112	117	118
line25	25	26	line69	72	73	line113	105	119
line26	26	27	line70	73	74	line114	119	120
line27	4	29	line71	74	75	line115	120	121
line28	29	30	line72	75	76	line116	121	122
line29	30	31	line73	76	77	line117	122	123
line30	31	32	line74	77	78	line118	48	27
line31	32	33	line75	78	79	line119	17	27
line32	33	34	line76	79	80	line120	8	24
line33	34	35	line77	67	81	line121	56	45
line34	35	36	line78	81	82	line122	65	56
line35	31	37	line79	82	83	line123	38	65
line36	37	38	line80	83	84	line124	9	42
line37	30	40	line81	84	85	line125	61	100
line38	40	41	line82	85	86	line126	76	95
line39	41	42	line83	86	87	line127	91	78
line40	42	43	line84	87	88	line128	103	80
line41	43	44	line85	82	89	line129	113	86
line42	44	45	line86	89	90	line130	110	89
line43	45	46	line87	90	91	line131	115	123
line44	46	47	line88	68	93	line132	25	36

REFERENCES

[1] S. S. Thale, R. G. Wandhare, and V. Agarwal, "A Novel Reconfigurable Microgrid Architecture with Renewable Energy Sources and Storage," IEEE Trans. Ind. Appl., vol. 51, no. 2, pp. 1805–1816, Mar. 2015.

[2] S. A. Abdelrazek and S. Kamalasadan, "Integrated PV Capacity Firming and Energy Time Shift Battery Energy Storage Management Using Energy-Oriented Optimization," IEEE Trans. Ind. Appl., vol. 52, no. 3, pp. 2607–2617, May 2016.

[3] P. U. Herath et al., "Computational Intelligence Based Demand Response Management in a Microgrid," IEEE Trans. Ind. Appl., pp. 1–1, 2018.

[4] J. Mitra, M. R. Vallem, and C. Singh, "Optimal Deployment of Distributed Generation Using a Reliability Criterion," IEEE Trans. Ind. Appl., vol. 52, no. 3, pp. 1989–1997, May 2016.

[5] L. Meng et al., "Flexible System Integration and Advanced Hierarchical Control Architectures in the Microgrid Research Laboratory of Aalborg University," IEEE Trans. Ind. Appl., pp. 1–1, 2015.

[6] K. Chen, W. Wu, B. Zhang, S. Djokic, and G. P. Harrison, "A Method to Evaluate Total Supply Capability of Distribution Systems Considering Network Reconfiguration and Daily Load Curves," IEEE Trans. Power Syst., vol. 31, no. 3, pp. 2096–2104, May 2016.

[7] J. Li, X.-Y. Ma, C.-C. Liu, and K. P. Schneider, "Distribution System Restoration With Microgrids Using Spanning Tree Search," IEEE Trans. Power Syst., vol. 29, no. 6, pp. 3021–3029, Nov. 2014.

[8] S. A. Arefifar, Y. A.-R. I. Mohamed, and T. H. M. EL-Fouly, "Comprehensive Operational Planning Framework for Self-Healing Control Actions in Smart Distribution Grids," IEEE Trans. Power Syst., vol. 28, no. 4, pp. 4192–4200, Nov. 2013.

[9] J. Ghorbani, M. A. Choudhry, and A. Feliachi, "A MAS learning framework for power distribution system restoration," in T&D Conference and Exposition, 2014 IEEE PES, 2014, pp. 1–6.

[10] J. Ghorbani, S. Chouhan, M. A. Choudhry, and A. Feliachi, "Hybrid multi agent approach for power distribution system restoration," in Energytech, 2013 IEEE, 2013, pp. 1–5.

[11] K. Chen, W. Wu, B. Zhang, and H. Sun, "Robust Restoration Decision-Making Model for Distribution Networks Based on Information Gap Decision Theory," IEEE Trans. Smart Grid, vol. 6, no. 2, pp. 587–597, Mar. 2015.

[12] H. Xiaoyu, X. Mingchao, and H. Yinghui, "A Service Restoration Method for Active Distribution Network," Energy Procedia, vol. 61, pp. 339–344, 2014.

[13] X. Chen, W. Wu, and B. Zhang, "Robust Restoration Method for Active Distribution Networks," IEEE Trans. Power Syst., vol. 31, no. 5, pp. 4005–4015, Sep. 2016.

[14] M. J. Ghorbani, M. A. Choudhry, and A. Feliachi, "A Multiagent Design for Power Distribution Systems Automation," IEEE Trans. Smart Grid, vol. 7, no. 1, pp. 329–339, Jan. 2016.

[15] S. Das, D. Das, and A. Patra, "Reconfiguration of distribution networks with optimal placement of distributed generations in the presence of remote voltage controlled bus," Renew. Sustain. Energy Rev., vol. 73, pp. 772–781, Jun. 2017.

[16] L. Xu, R. Cheng, Z. He, J. Xiao, and H. Luo, "Dynamic Reconfiguration of Distribution Network Containing Distributed Generation," in 2016 9th International Symposium on, 2016, vol. 1, pp. 3–7.

[17] O. K. Siirto, A. Safdarian, M. Lehtonen, and M. Fotuhi-Firuzabad, "Optimal Distribution Network Automation Considering Earth Fault Events," IEEE Trans. Smart Grid, vol. 6, no. 2, pp. 1010–1018, Mar. 2015.

[18] M. Eriksson, M. Armendariz, O. O. Vasilenko, A. Saleem, and L. Nordstrom, "Multiagent-Based Distribution Automation Solution for Self-Healing Grids," IEEE Trans. Ind. Electron., vol. 62, no. 4, pp. 2620–2628, Apr. 2015.

[19] S. Lei, J. Wang, and Y. Hou, "Remote-Controlled Switch Allocation Enabling Prompt Restoration of Distribution Systems," IEEE Trans. Power Syst., vol. 33, no. 3, pp. 3129–3142, May 2018.

[20] J. C. López, M. J. Rider, A. V. Garcia, P. L. Cavalcante, L. F. Miranda, and L. L. Martins, "Optimization approach for the allocation of remote-controlled switches in real-scale electrical distribution systems," in Innovative Smart Grid Technologies Conference Europe (ISGT-Europe), 2017 IEEE PES, 2017, pp. 1–6.

[21] S. Lei, Y. Hou, F. Qiu, and J. Yan, "Identification of Critical Switches for Integrating Renewable Distributed Generation by Dynamic Network Reconfiguration," IEEE Trans. Sustain. Energy, vol. 9, no. 1, pp. 420–432, Jan. 2018.

[22] A. M. Tahboub, V. R. Pandi, and H. H. Zeineldin, "Distribution System Reconfiguration for Annual Energy Loss Reduction Considering Variable Distributed Generation Profiles," IEEE Trans. Power Deliv., vol. 30, no. 4, pp. 1677–1685, Aug. 2015.

[23] M. A. Elgenedy, A. M. Massoud, and S. Ahmed, "Smart grid self-healing: Functions, applications, and developments," in Smart Grid and Renewable Energy (SGRE), 2015 First Workshop on, 2015, pp. 1–6.

[24] Z. Lin, F. Wen, and Y. Xue, "A Restorative Self-Healing Algorithm for Transmission Systems Based on Complex Network Theory," IEEE Trans. Smart Grid, vol. 7, no. 4, pp. 2154–2162, Jul. 2016.

[25] J. M. Andújar, F. Segura, and T. Domínguez, "Study of a renewable energy sources-based smart grid. requirements, targets and solutions," in Power Engineering and Renewable Energy (ICPERE), 2016 3rd Conference on, 2016, pp. 45–50.

[26] J. B. Leite and J. R. S. Mantovani, "Development of a Self-Healing Strategy With Multiagent Systems for Distribution Networks," IEEE Trans. Smart Grid, vol. 8, no. 5, pp. 2198–2206, Sep. 2017.

[27] R. Gupta, D. K. Jha, V. K. Yadav, and S. Kumar, "A multi-agent based self-healing smart grid," in Power and Energy Engineering Conference (APPEEC), 2013 IEEE PES Asia-Pacific, 2013, pp. 1–5.

[28] Y. Xu, C.-C. Liu, K. P. Schneider, and D. T. Ton, "Placement of Remote-Controlled Switches to Enhance Distribution System Restoration Capability," IEEE Trans. Power Syst., vol. 31, no. 2, pp. 1139–1150, Mar. 2016.

[29] R. E. Brown, "Impact of smart grid on distribution system design," in Power and Energy Society General Meeting-Conversion and Delivery of Electrical Energy in the 21st Century, 2008 IEEE, 2008, pp. 1–4.

[30] M. Sperandio, J. Coelho, and C. C. B. Carmargo, "Automation planning of loop controlled distribution feeders," in 2nd International Conference on Electrical Engineering (CEE'07), 2007.

[31] L. L. Pfitscher, D. P. Bernardon, L. N. Canha, V. F. Montagner, V. J. Garcia, and A. R. Abaide, "Intelligent system for automatic reconfiguration of distribution network in real time," Electr. Power Syst. Res., vol. 97, pp. 84–92, Apr. 2013.

[32] N. G. Paterakis et al., "Multi-Objective Reconfiguration of Radial Distribution Systems Using Reliability Indices," IEEE Trans. Power Syst., vol. 31, no. 2, pp. 1048–1062, Mar. 2016.

[33] C. S. Chen, C. H. Lin, H. J. Chuang, C. S. Li, M. Y. Huang, and C. W. Huang, "Optimal Placement of Line Switches for Distribution Automation Systems Using Immune Algorithm," IEEE Trans. Power Syst., vol. 21, no. 3, pp. 1209–1217, Aug. 2006.

[34] S. Ray, A. Bhattacharya, and S. Bhattacharjee, "Optimal placement of switches in a radial distribution network for reliability improvement," Int. J. Electr. Power Energy Syst., vol. 76, pp. 53–68, Mar. 2016.
[35] S. Ray, S. Bhattacharjee, and A. Bhattacharya, "Optimal allocation of remote control switches in radial distribution network for reliability improvement," Ain Shams Eng. J., vol. 9, no. 3, pp. 403–414, Sep. 2018.
[36] D. P. Bernardon, A. P. C. Mello, L. L. Pfitscher, L. N. Canha, A. R. Abaide, and A. A. B. Ferreira, "Real-time reconfiguration of distribution network with distributed generation," Electr. Power Syst. Res., vol. 107, pp. 59–67, Feb. 2014.
[37] S.F. Santos, D.Z. Fitiwi, M. Shafie-khah, A.W. Bizuayehu, C.M.P. Cabrita, J.P.S. Catalão, "New multi-stage and stochastic mathematical model for maximizing RES hosting capacity—Part I: problem formulation", IEEE Transactions on Sustainable Energy, Vol. 8, No. 1, pp. 304-319, January 2017
[38] Jakub Nowotarski, Rafał Weron, "Recent advances in electricity price forecasting: A review of probabilistic forecasting", Renewable and Sustainable Energy Reviews, Vol. 81, Part 1, 2018.
[39] Tao Hong, Jingrui Xie, Jonathan Black, "Global energy forecasting competition 2017: Hierarchical probabilistic load forecasting", International Journal of Forecasting, 2019.
[40] Lei Xu, Shengwei Wang, Rui Tang, "Probabilistic load forecasting for buildings considering weather forecasting uncertainty and uncertain peak load", Applied Energy, Vol. 237, pp. 180-195, 2019.
[41] Zhifeng Guo, Kaile Zhou, Xiaoling Zhang, Shanlin Yang, "A deep learning model for short-term power load and probability density forecasting", Energy, Vol. 160, pp. 1186-1200, 2018.
[42] C. Lee, C. Liu, S. Mehrotra, and Z. Bie, "Robust Distribution Network Reconfiguration," IEEE Trans. Smart Grid, vol. 6, no. 2, pp. 836–842, Mar. 2015.
[43] S. F. Santos, D. Z. Fitiwi, M. R. M. Cruz, C. M. P. Cabrita, and J. P. S. Catalão, "Impacts of optimal energy storage deployment and network reconfiguration on renewable integration level in distribution systems," Appl. Energy, vol. 185, pp. 44–55, Jan. 2017.
[44] C. Santos, S. F. Santos, D. Z. Fitiwi, M. R. Cruz, and J. P. Catalão, "Sensitivity Analysis in Switches Automation Based on Active Reconfiguration to Improve System Reliability Considering Renewables and Storage," in 2018 IEEE International Conference on Environment and Electrical Engineering and 2018 IEEE Industrial and Commercial Power Systems Europe (EEEIC/I&CPS Europe), 2018, pp. 1–6.

Sergio F. Santos received the B.Sc., M.Sc. and Ph.D. degrees from the University of Beira Interior (UBI), Covilhã, Portugal, in 2012, 2014 and 2017, respectively. His research interests include planning and operation of distribution systems, and smart grid technologies.

Desta Z. Fitiwi received the Ph.D. degree in Sustainable Energy Technologies and Strategies (SETS), jointly offered by Comillas Pontifical University, KTH and Delft University of Technology, in 2016. His research interests include regulation and economics of the power industry, transmission expansion planning, sustainable energy modeling and strategic planning.

Marco R. M. Cruz received the M.Sc. degree from the Faculty of Engineering of the University of Porto (FEUP), Porto, Portugal, in 2016, and the Ph.D. degree from the University of Beira Interior (UBI), Covilhã, Portugal, in 2019. His research interests include planning and operation of distribution systems, and smart grid technologies.

Cláudio Santos received the M.Sc. degree from the Faculty of Engineering of the University of Porto (FEUP), Porto, Portugal, in 2018. His research interests include distribution systems, system reliability, renewables and energy storage.

João P. S. Catalão (M'04-SM'12) the Ph.D. degree and Habilitation for Full Professor ("Agregação") from the University of Beira Interior (UBI), Covilha, Portugal, in 2007 and 2013, respectively. His research interests include power system operations and planning, distributed renewable generation, demand response and smart grids.